# A MECHANICS-BASED PROCEDURE TO DETERMINE THE DAMAGE MECHANISM OF MASONRY WALLS SUBJECTED TO OUT-OF-PLANE HORIZONTAL LOADINGS

## V. Putrino[(1)], D. D'Ayala[(2)]

[(1)] *PhD Student, University College London, v.putrino@ucl.ac.uk*
[(2)] *Professor of Structural Engineering, University College London, d.dayala@ucl.ac.uk*

*Abstract*

Masonry buildings are among the most widespread building typologies around the world, very often located in multi-hazard-prone regions. Although well-built masonry structures have proven to survive for centuries even in areas struck by natural perils, the majority of them are perceived very vulnerable due to their low-engineered construction features. To date, many research efforts have been devoted to thoroughly investigate the mechanism of failure of masonry structures subjected to seismic loading. Several methods have been developed and computationally demanding software systems have been employed to attempt the most accurate detection of crack patterns and failure modes. However, similar efforts currently lack in the understanding of how these structures behave when subjected to other loading profiles, such as the ones exerted by flooding or high-winds speed. In addition, when trying to assess the vulnerability of large populations of masonry structures, heavy computations require resources very often not affordable, thus highlighting the need of having more simplified yet reliable procedures able to satisfactorily support rapid decision-making processes. This paper presents a mechanics-based procedure (MB_P) for the collapse load evaluation and failure mechanism identification of masonry walls subjected to seismic, flood and wind loading profiles. This method is based on Yield Line Theory and incorporates several adjustments to account for the interaction between masonry units and mortar and how this can affect the determination of the collapse mechanisms and the position of maximum displacement. The results of the application of the method to a single wall undergoing the three mentioned types of loading are presented of the point of convergence of the crack lines. The paper concludes with a comparison between the results obtained via the application of the proposed analytical procedure and the results obtained by using the commercial structural analysis software ELS (Extreme Loading for Structures) based on the Applied Element Method (AEM).

*Keywords: Masonry Structures, Multi-hazard Assessment, Quantitative Analytical Procedure, Failure Mechanism.*

## 1. Introduction

Masonry buildings are among the most distinctive and valuable building typologies worldwide, often representing a very important component of individual and collective cultural identity. Given their widespread use since ancient times, these structures are also recognized to possess cultural value and universal significance but also perceived to be very vulnerable to natural destructive events.

Considering the rapid changes recently recorded in climate conditions [1], it is becoming of increasing importance to advance methods and techniques to assess the vulnerability of buildings subjected to multiple or even co-occurring natural events, which are characterized by very different features and exert their action to buildings in different ways.

There is currently a considerable discrepancy between the level of understanding and the detail of analysis achieved for the structural assessment of buildings exposed to different hazards, such as earthquake, wind or flood.

Numerous studies are available in the field of seismic vulnerability assessment of non-engineered structures [2], while works in the field of flood and wind vulnerability assessment are still very modest, challenging the development of comprehensive analytical methods able to conduct multi-hazard vulnerability assessment and to carry out the analysis in a commensurate manner across these hazards while also being able to rank the results on the basis of a single common scale [3].

When performing multi-hazard vulnerability assessment, it is of fundamental importance to consider not only the mutual interactions between the single perils considered [4], but also to understand how to correlate the

results to guarantee a meaningful comparison [3]. There are currently two main frameworks that can be followed, namely 1) multi-layer single-hazard assessment approach (i.e. the events are assessed individually and the results do not account for any interaction/overlap of events [5], or 2) multi-hazard assessment approach, which considers both the simultaneous interdependency of events which occur within the same area and time window as well as the cascading events, i.e. when a given event may trigger a secondary event and consequences are inter-related. Among the studies included in literature, the work in [5] provides an independent treatment of the hazard assessment models linked through a 'pinch point' variable. This is a generic concept that can be applied to any set of structures affected by any set of hazards, as long as the chosen analytical method is able to represent the response of the structure under different loading profiles by means of one single analytical parameter representative of the structure response which is independent of the type of loading considered. Hence the n-hazards can be kept separate (i.e. adoption of type 1) approach) and then compared in terms of probability of damage caused to the assets' typology due to their impact.

With regards to the available analytical methods to conduct multi-hazard vulnerability assessment of masonry walls, one of the current limitations encountered in literature relates to the ability of the model to determine the effects of seismic action on the structures but rarely the actions of other hazards. Simplified macro-element models based on Yield Line (YL) Theory [6] which are based on kinematic principles and characterized by limited number of parameters needed to determine the limit of collapse of structures [7] proved their efficacy in multi-hazard frameworks. Several studies report their use to conduct seismic [2] and flood vulnerability assessment [8][9] of brick and stone masonry structures; experimental studies are also available to validate analytical works based on YL concepts such as the ones conducted by [10] and by [11] respectively in the field of seismic and flood vulnerability. Works on wind vulnerability assessment are currently focused on assessing damage to building components (i.e. roof and roof elements) rather than on structural walls, however [12] have conducted experimental tests on scaled models to determine the ultimate load capacity, the crack pattern at failure and the identification of processes that occur under increasing uniform wind lateral loading simulated by air bags acting against the wall. Macro-modelling approaches are generally preferred to more detailed micro-modelling approaches as they are less computationally demanding in terms of time and resources needed to build the models and to run the analysis, thus facilitating the assessment of large portfolios of buildings [13].

In this study, a mechanics-based procedure (MB_P) to determine the damage mechanism of masonry structures subjected to horizontal seismic, flood and wind loadings is proposed and presented in Section 2. The procedure is based on plastic analysis principles and, starting from the YL Theory concepts, adds up additional layers of complexity to include the contribution of torsional effects caused by the application of horizontal loading to the structure. The procedure is part of a wider framework, aimed at conducting a full comparative assessment through the derivation of single-hazards fragility curves which are used to compare the damage extent caused by the three perils considered [14]. The proposed multi-hazard vulnerability assessment framework is described in its entirety, with specific focus on the analytical method proposed to define the parameters (collapse load factor and performance variable) able to correlate the hazard profiles to the structural damage of masonry walls. The developed analytical model is applied to a wall undergoing seismic, flood and wind loadings to show the feasibility of the approach and the ease of comparability between different hazards; the geometric and material properties affecting the trends of λ values are reported in Section 3. Finally, results are compared with the output of micro modelling analysis using a Discrete Element Method software defined as Extreme Loading for Structure (ELS), in terms of crack pattern and consequent position of the point of convergence of the yield lines (YLs) for which maximum displacement is attained, to discuss the reliability of the method when compared to computationally more expensive means of analysis; this comparison is reported in Section 3.2. Finally, conclusions are drawn in Section 4.

## 2. Proposed framework for multi-hazard vulnerability of masonry structures

The MB_P proposed in this work is shown in Fig. 1 Step 1 and 2 relate to the determination of the intensity measures (defined deterministically) and the exposure data needed to conduct full risk assessment analysis. These steps feed into step 3, which details the kinematic analytical model developed to conduct the assessment of masonry structures subjected to out-of-plane loading.
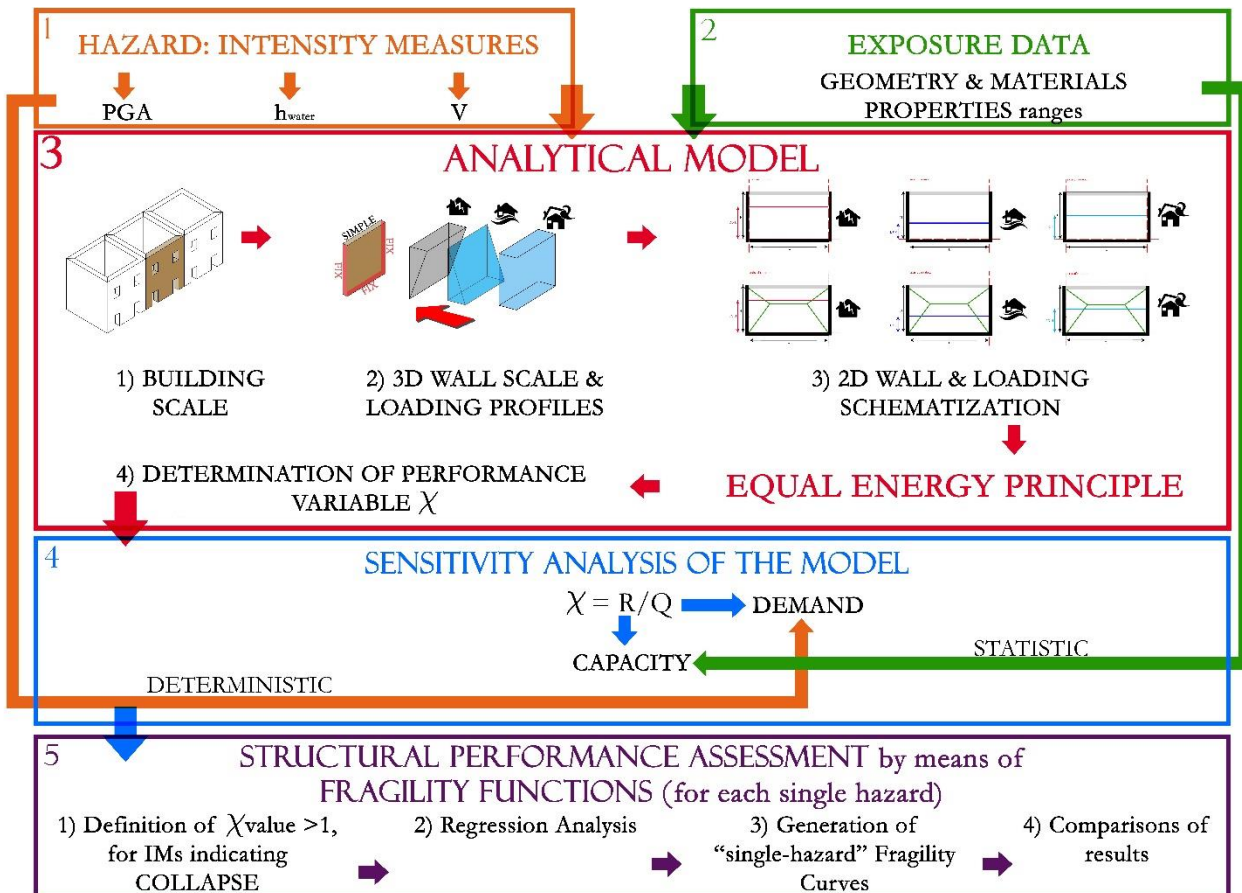
Fig. 1 – General framework for multi-hazard vulnerability assessment of masonry structures

The assessment is conducted at wall scale. From the 3D building scale, a 2D model is obtained by simply considering each masonry unit as an assembly of individual walls, each characterized by its own set of boundary conditions and opening layout (size and position). Depending on the position of building wall considered (i.e. individual building or within a cluster), various combinations of 4-sides-restrained or 3-sides-restrained walls can be defined. The degree of restrain provided by the presence of horizontal structures (i.e. roof and/or floors) is simulated by different levels of fixity of the horizonal edges of the walls. The loading profiles are applied individually to the wall (thus adopting type 1) approach mentioned in Introduction), and "simplified" as knife edge loads applied at different positions of the wall. This assumption facilitates the determination of the set of equations needed to determine the External Work $W_e$ for each case, which, as far as the magnitude of the load is concerned, will only depend on its position with respect to the base of the wall. A crack pattern for each wall layout will be assumed, which must be compatible with restraints and loading profiles. Revisited YL Theory concepts including the contribution of torsional moments are used to analyze each individual specimen, producing a limit state analysis which identifies the value of loading that determines the collapse for a given set of boundary conditions. An optimization routine is created to find the minimum multiplier of the load to be applied to produce failure, resulting in a specific collapse load pattern and a value of collapse load factor, defined as λ factor. As the λ factor is found, the corresponding position of maximum displacement of the point of convergence of vertical, horizontal and diagonal crack lines gets defined, as a proportion of wall height. In analytical terms, the λ factor is found by applying the Virtual Work Method to the Mechanism Approach and by equating the work done by external forces (i.e. the ultimate load λq which causes collapse) to the internal capacity of the wall, as shown in Eq. (1), given as a sum of vertical and horizontal moment capacity as shown in Eq. (2):

$$W_e = W_i \tag{1}$$

$$\lambda q \, K_1 = (M_h + M_v)K_2 \tag{2}$$

$K_1$ and $K_2$ indicate respectively the remaining terms defining Eq. (2), namely the lengths of the KEL portions and the linear displacements, and the length of the cracks and the virtual rotation (i.e. the rotation undertaken by the crack lines when subjected to the given horizontal loading).

$$\lambda = \frac{(M_h + M_v)K_2}{qK_1} \tag{3}$$

While the value of $q$ depends on the loading considered and is a case-dependent variable of the Eq. (3), as far as the geometric and material characteristics of the wall are defined, the components defining the capacity of the wall remain constant throughout each assessment.

The capacity in vertical direction $M_v$ is defined as a function of the flexural tensile strength of the mortar along the bed joint, and the axial stress given by the self-weight of the wall [15], as shown in Eq. (4)

$$M_v = (f_{xk1} + \sigma_{wall}) \tag{4}$$

The horizontal component of the moment capacity in Eq. (3) is instead defined as a sum of the shear strength component $M_{Htorsion}$ and the flexural strength component $M_{Hflexure}$. The former is given in Eq. (5)

$$M_{Htorsion} = k_b \tau_{um} t^3 \tag{5}$$

The shear moment capacity in Eq. (5) is a function of the dimensionless torque coefficient factor $k_b$, the shear strength of the bond $\tau_{um}$ and the thickness of the wall.

The latter, as defined in [15], is reported in Eq. (6)

$$M_{Hflexure} = f_{xk2} Z \tag{6}$$

The flexure component of the horizontal moment capacity in Eq. (6) is a function of the flexural tensile strength perpendicular to the bed joint and the section modulus of the plan shape of the wall.

The moment capacities presented in Eq. (4), (5), (6) are computed at brick level.

From the definition of the $\lambda$ factor, the structural performance variable $\chi$ can be determined, namely the ratio between Demand (Q) imposed by the load and Capacity (R) of the system, else interpretable as the inverse of the load multiplier.

$$\chi = \frac{W_e}{W_i} = \frac{1}{\lambda} \tag{7}$$

Each $\chi$ values indicates the response of the wall for the given IM considered, thus representing the analytical parameter needed to link the hazard component to the damage caused to the structural system considered, fundamental for the derivation of fragility curves.

Considering the challenges in defining limit states performance criteria which can easily allow the damage comparison across all three hazard scenarios, only the limit state of collapse is herein considered. More specifically, the structural limit state of collapse is described as the critical value of PGA, floodwater depth ($h_{water}$) and wind speed (V) corresponding to $\chi = 1$, i.e. when Demand is equal to Capacity.

The assumption of a scenario approach implies that the Demand imposed on the system is deterministically known. The probability of failure ($P_f$) of the system (i.e. wall) is defined as the probability that the Demand (Q) is greater than the Capacity (R), which, as shown in Fig.1, results in having $\chi > 1$ Eq. (8):

$$P_f = \Pr(R/Q) > 1) \tag{8}$$

If the Demand is treated/assumed as deterministic, the only source of variability considered in this study relates to the Capacity (R), therefore involving the geometric and material parameters of the wall. Step 4 of the proposed framework focuses on verifying the performance levels and consequent values of structural performance variable $\chi$ for different "families" of walls (i.e. each "family" refers to a given set of boundary conditions of the wall layout considered) by conducting a sensitivity analysis of the parameters affecting the moment capacity of the system, which are made to vary within given ranges obtained either from the literature, from experimental testing or site investigations. In particular, the "nominal range sensitivity analysis" (NRSA) is used, to evaluate the effect of each variable varying within given ranges [16]. The general framework concludes with the derivation of single-hazard fragility curves, defined as the probability of

4

reaching/exceeding collapse for a given IM and derived as a function of PGA, floodwater depth ($h_{water}$) and wind speed (V) for each "family" of walls introduced in Step 3. The identification of the walls' failure modes and correspondent χ will ensure the comparison between obtained results and ultimately, the determination of the most damaging scenario among the ones considered. Following section will focus on describing in more detail step 3 of the framework.

## 3. Application of the proposed analytical model

To the aim of verifying the analytical model proposed to conduct multi-hazard vulnerability assessment, a brick masonry wall is used, simply restrained on all 4 edges, with no openings and no additional loadings applied except its self-weight. The geometric and material properties defining the wall are reported in Table 1.

Table 1 – Geometrical and Material Characteristics of the wall

| Wall Parameter | Mean Value | Range | Unit |
|---|---|---|---|
| Wall Length | 4.5 | 3.0 – 6.0 | m |
| Wall Height | 3.0 | 2.0 – 5.0 | m |
| Wall thickness | 0.13 | 0.10 – 0.50 | m |
| Brick Unit Length | 0.25 | 0.10 – 0.30 | m |
| Brick Unit Height | 0.075 | 0.10 – 0.25 | m |
| Mortar Joint Thickness | 0.01 | -- | m |
| Density of brick | 19 | -- | kN/m$^3$ |
| Flexural tensile strength parallel to bed joint ($f_{xk1}$) | 0.52 [10] | 0.10 – 0.60 | MPa |
| Flexural tensile strength orthogonal to bed joints ($f_{xk2}$) | 2.08 [15] | 4*($f_{xk1}$) | MPa |
| Friction coefficient | 0.576 [17] | 0.20 – 0.60 | -- |

The three loading profiles (i.e. seismic, flood and wind) are schematically applied to the wall as "simplified" knife edge loads (KELs), with line of application inferred from the loading shape, as reported in Table 2. The equations to determine the value of $\lambda q$ and the value of IM chosen to obtain the same order of magnitude of the three loadings is also shown, to allow for the following results to be compared. The only exception is represented by the wind loading, for which a value of 75 m/s corresponding to Category 5 in the Saffir-Simpson Hurricane Wind Scale is adopted [18].

Table 2 – Loading profiles: seismic, flood and wind

| Loading type | Height of KEL application | Load Value | Reference intensity of hazard action | Value (kN/m) |
|---|---|---|---|---|
| $q_{seismic}$ | 2/3 H | $q_{seimsic} = \lambda(a\ H\ t\ \rho_{brick})$ | a = 1 g | 46.60 |
| $q_{flood}$ | 1/3 h water | $q_{flood} = \lambda(1/2\ g\ h^2\ \rho_{water})$ | h water = H wall | 44.15 |
| $q_{wind}$ | 1/2 H | $q_{wind} = \lambda(1/2\ V^2\ H\ C\ \rho_{air})$ | V = 75 m/s | 10.54 |

As the KELs are applied along the height of the wall, a feasible crack pattern is then assumed in accordance with the boundary conditions. For each wall configuration, a minimum of two feasible crack patterns can be assumed. However, the "critical" pattern, namely the one which requires the least work for its formation, will be the one for which the collapse load factor λ is the minimum, also corresponding to the pattern in which the

5

convergence point of all crack lines will involve the greatest wall portion in the mechanism. The two patterns hypothesized for each loading profile are presented in Table 3.

Table 3 – Crack patterns identified for seismic, flood and wind KELs

| Crack Pattern 1_A | Crack Pattern 1_B | Crack Pattern 1_C | Crack Pattern 2_A | Crack Pattern 2_B | Crack Pattern 2_C |
|---|---|---|---|---|---|
|  |  |  |  |  |  |
|  |  |  |  |  |  |
|  |  |  |  |  |  |

Each of the patterns presented in Table 3 is characterized by three different phases, namely A, B, and C, which aim at clarifying the interaction between cracks and KEL. In order to find the "correct" pattern, several iterations are required. While at each iteration, the internal moment capacity does not vary, the action caused by the KELs portions will change in accordance with the specific configuration of cracks considered. Since the boundary conditions are symmetrical, assumptions are required when defining the length of both the vertical crack line in CP1 and the horizontal crack line in CP2. Similarly, the two symmetric points of convergence of diagonal crack lines are assumed to be located at a maximum distance set to be as follows:

- When considering CP1s, the lower point of convergence (i.e. 1) can move up to a maximum wall height equal to the line of application of the KEL, namely 2/3 H for seismic KEL, 1/3h for flood KEL, 1/2 H for wind KEL. The upper point of convergence (i.e. 2) will be located at 2/3 H wall. According to this assumption, the length of the vertical YL will be equal to 0 for seismic KEL, 1/3 H for flood KEL and 1/6 H for wind KEL.
- When considering CP2 the position of point 3 and 4 is set to reach a maximum length of L/2; if $x$ is the distance between the vertical side of wall and the point of max displacement, at each iteration the its value will be equal to:

$$x = y_i \tan \alpha$$

(9)

with $y_i$ being each step of the wall (i.e. each brick course of wall) and $\alpha$ being the angle forming between the lower orthogonal sides of the wall.

Following sections present the results of crack patterns' comparison in terms of λ values obtained for each loading profile assessed individually, followed by a discussion of the "critical" crack patterns of all three loadings considered.

## 3.1 Comparisons of CP1 and CP2 for each loading profile

Fig 2 a) b) and c) show the λ – y/H curves (i.e. position of maximum displacement of the point of convergence of cracks normalized to the H of the wall) for seismic, flood and wind loading assessed individually; a summary of obtained results is reported in Table 4. The comparison of crack patterns reported in Fig 2 highlights that CP1 is the "critical" in all three cases considered.
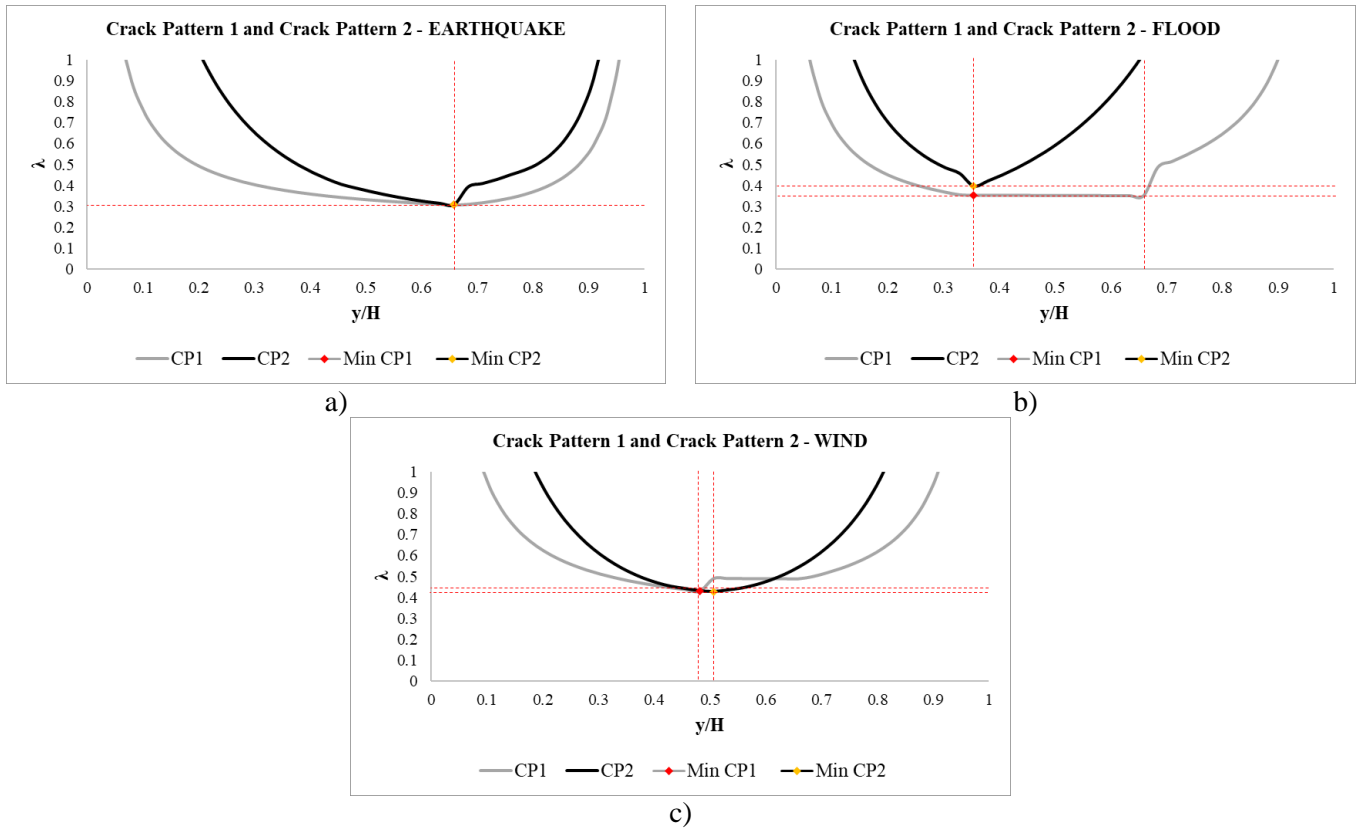
6

a)



b)



c)

Fig 2 - Comparison between CP1 and CP2 for a) seismic, b) flood, c) wind

Table 4 – Comparison between CP1 and CP2 for seismic, flood and wind loadings

| Loading | CP1 Min λ | CP1 y/H | CP2 Min λ | CP2 y/H |
|---------|-----------|---------|-----------|---------|
| Earthquake | 0.308 | 0.659 | 0.309 | 0.659 |
| Flood | 0.352 | 0.658 | 0.396 | 0.355 |
| Wind | 0.431 | 0.481 | 0.428 | 0.507 |

The values reported in Table 4 show that there is a considerable discrepancy in terms of Min λ values and position of maximum displacement of the point where the crack lines converge in the case of flood loading.
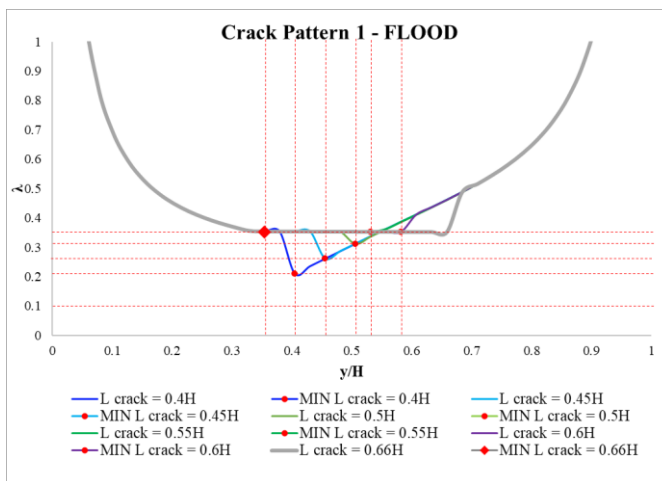


| Case | Min λ | y/H |
|------|-------|-----|
| L crack = 0.40 H | 0.209 | 0.405 |
| L crack = 0.45 H | 0.261 | 0.456 |
| L crack = 0.50 H | 0.312 | 0.507 |
| L crack = 0.55 H | 0.353 | 0.532 |
| L crack = 0.60 H | 0.353 | 0.583 |

Fig 3 – Variation in λ and y/H values for different lengths of vertical crack line and summary table

7

It appears evident that, although imposing a length of vertical crack equal to 1/3H for CP1 results in a smaller value of λ in comparison to CP2, it can be observed that the displacement of the whole vertical line running from 1/3 H to 2/3 H is the same, hence the same Min λ is registered. To the aim of verifying the validity of the assumptions made on the crack pattern CP1, a sensitivity analysis is conducted to evaluate the influence of the parameter length of vertical crack on the resulting Min λ and y/H values in CP1 for the case of flood, when varying across the range comprised between 1/3 H and 2/3 H. The λ - y/H curves presented in Fig 3 – Variation in λ and y/H values for different lengths of vertical crack lineclearly demonstrate the relevance of the parameter "length of vertical crack line" within the overall determination of the Min λ for CP1. This demonstrate that, in a multi-hazard framework dealing with different types of loading, it is required to define set of assumptions very often tailored on a loading-by-loading basis. More specifically, a length of vertical crack comprised within the range of 0.33H and 0.4H is the one that provides with the lowest Min λ among the various vertical crack lengths considered.
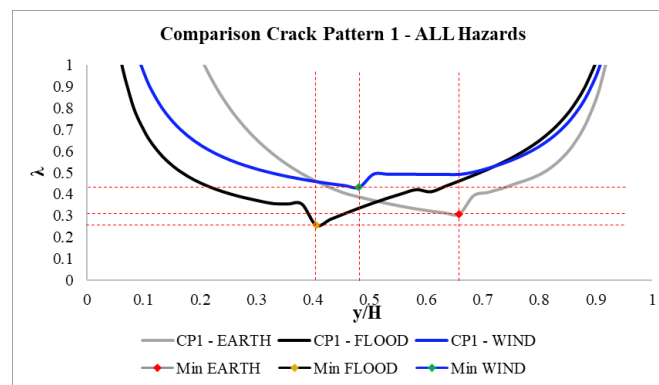


Fig 4 – Comparison of CP1 for all hazards

Fig 4 – Comparison of CP1 for all hazards provides the comparison of λ - y/H curves, Min λ and maximum cracks' convergence point of displacement for seismic, flood and wind KEL. It is important to note that the flood curve used in this comparison is the one generated by using a length of vertical crack for CP1 comprised between 0.33 H and 0.40 H. Table 5: Min λ and y/H values for seismic, flood and wind loading considering CP1 provides a summary of results obtained.

Table 5: Min λ and y/H values for seismic, flood and wind loading considering CP1

| Loading | Min λ | y/H |
|---|---|---|
| Earthquake | 0.308 | 0.659 |
| Flood | 0.209 | 0.405 |
| Wind | 0.431 | 0.481 |

In accordance with Fig 4 and Table 5, the wall shows to have minimum resistance to the flood loading, with point of maximum displacement involving 40% of the wall's height. In comparison to the seismic loading, the scatter between λ values is comparatively very small, while the portion of wall involved in the mechanism almost duplicate. The wind loading is the least probable to activate the mechanism among the three perils, as it is characterized by the highest value of λ. The graphs reported in Figure 5 show the influence of global, local and material parameters on the determination of the λ factor, with mean values marked with blue dots. To the aim of comparing the influence of the wind loading with respect to flood and seismic loading, it is chosen to extend the range up to 2, although a threshold of 1 is marked to highlight the only meaningful results to consider. From Figure 5 a) it is possible to observe that for γ values greater than 1 (i.e. indicating the condition in which the length of the wall becomes greater than the height of the wall) the flood loading is the one causing the wall to damage prior than other loadings considered. In no occasion the wind loading would cause the wall

8

to fail. As expected, walls made of longer brick units (i.e. $l_{unit}/h_{unit}= \kappa$, shown in Figure 5 b)) require a greater load magnitude to get to the collapse state; in only one case (i.e. for walls with a length of brick equal to 0.01 m the wall would experience failure, however the min $\lambda$ for this only case is almost eight times bigger than the ones of flood and seismic loading; the influence of flexural tensile strength plays a much more important role in determining the capacity of the wall, even at low magnitudes of loading applied, thus stressing its importance in comparison to geometric characteristics, as shown in Figure 5 c).
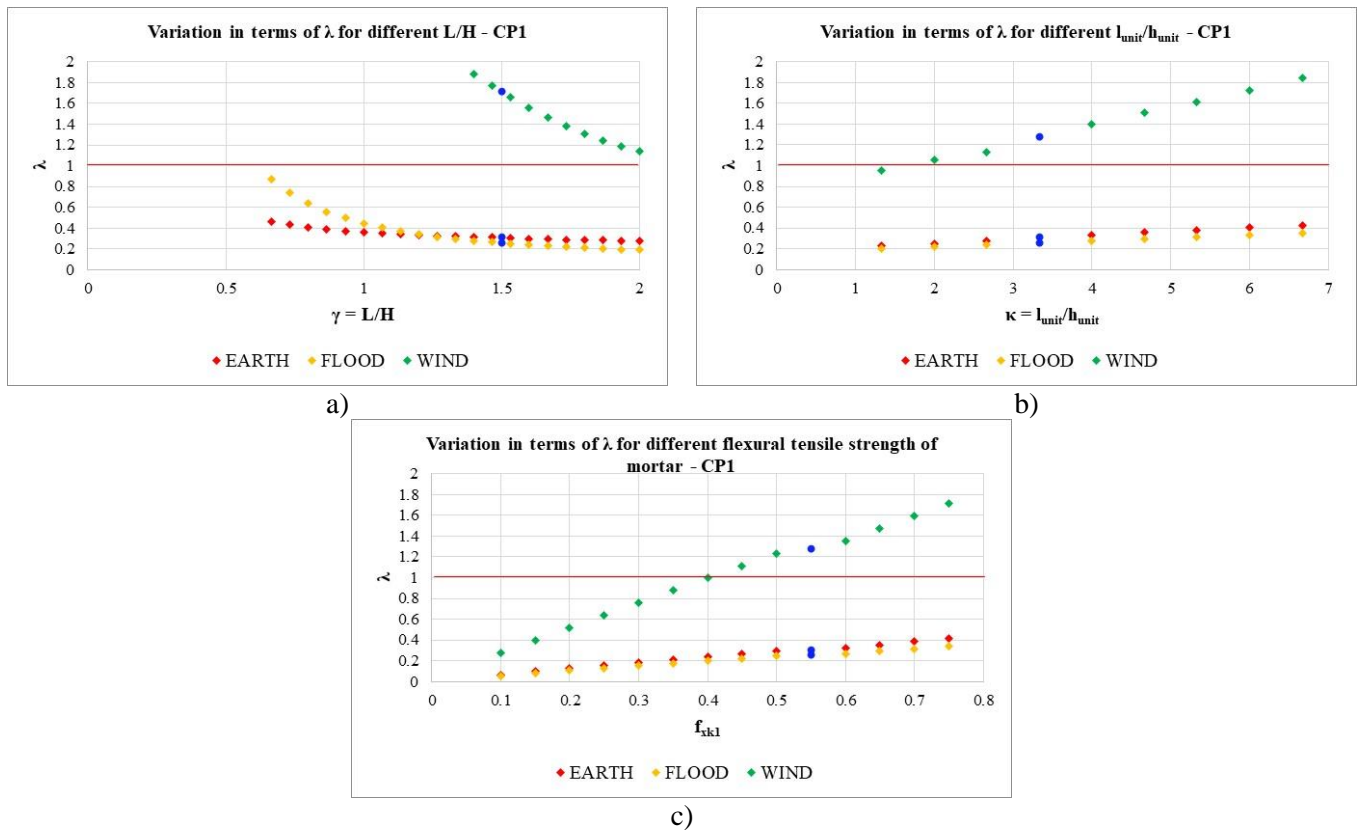


a)



b)



c)

Figure 5: a) Sensitivity to global geometric ratio L/H; b) Sensitivity to local geometric ratio $l_{unit}/h_{unit}$; c) Sensitivity to material parameter $f_{xk1}$

The results presented in this section assume that the pre-defined pattern is constituted by cracks running across the full length and height of the wall and an assumed height of water equal to the total height of the wall. However, especially when dealing with flood loading, such an assumption could present some flows. It could be also possible to obtain Min $\lambda$ for smaller water heights, also corresponding to different crack patterns initially hypothesized. Given these premises, a comparison is made between the behaviour of the wall undergoing flood loading simulated both with the proposed procedure and a simplified micro-modelling approach with the applied element method commercialized in Extreme Loading for Structures (ELS) software [19]. This comparison is presented in following section.

### 3.2 Comparison of proposed MB_P and ELS model – flood loading

The wall modelled in ELS is characterized by the same geometric and material characteristics used in previous comparisons and presented in Table 1. In the simplified micro-modelling approach, the mortar layer and the two-unit-mortar interfaces are lumped into a zero-thickness joint: this justifies the very small value of thickness of the joint chosen in this study (i.e. 0.001 m). One main difference between the two approaches is the treatment of the mortar joint connecting the masonry units. In the case of the M_B procedure proposed, the resistance in the vertical direction is provided by the flexural tensile strength (i.e. $f_{xk1}$ mentioned in Eq. (4)), a proportion of which constitutes the flexural strength in the perpendicular direction (i.e. $f_{xk2}$ mentioned in Eq. (6)) which are the two main contributors of the wall moment capacity. As soon as the internal moment capacity is overcome

9

by the external loading, the wall reaches collapse. In ELS, the interaction among the blocks is simulated by a number of deformable springs, namely, the "joint" springs representing the mortar plus unit-mortar interfaces and the "unit" springs, which guarantee the continuity within the units; these springs are characterized by force-displacement laws able to capture both the elastic and the post-elastic behavior of the material as a whole [20].The main aim of the comparison analysis is to verify at which height of the water (i.e. "critical" h) the crack pattern fully develops, which corresponds to finding λ=1 in the MB_P. In addition, the height of the point of maximum displacement of the converging crack lines will be compared, which highlights the different accuracy achieved by the two approaches. Since ELS computes the crack pattern in accordance with the increment of water height considered, the MB_P is revised in such a way that the pre-assumed crack pattern will only develop within the portion of wall subjected to the loading rather than running across the full height of the wall. This ensures a more precise estimation of the internal wall moment capacity, a more refined computation of the length of cracks, which also affects the estimation of the rotations of the wall portions bounded by the cracks and the displacements which the portions of KEL will undergo.
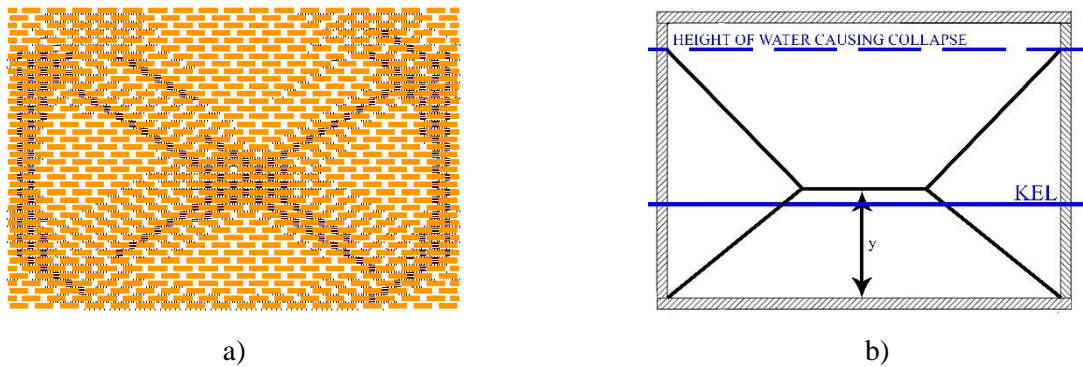


a)                         b)

Fig. 6: Comparison of crack patterns: a) ELS and b) MB_P

Fig. 6: Comparison of crack patterns: a) ELS and b) MB_P show the two crack patterns obtained from ELS and the MB_P respectively, which appear very similar in shape. However, since ELS is able to model the post-elastic behaviour of masonry, the crack pattern is more widely distributes thus indicating which springs have failed (i.e. black shades between brick units in Fig. 6: Comparison of crack patterns: a) ELS and b) MB_P a)) and which springs are undergoing large displacement (i.e. light shades between bricks units in Fig. 6: Comparison of crack patterns: a) ELS and b) MB_P a)).

İn terms of height of the water causing collapse and position of maximum displacement y, results are reported in Table 6. Even though the wall modelled in ELS is a 4-sides simply supported case, the presence of springs in the two orthogonal directions prevent the complete out-of-plane failure due to a residual in-plane tensile strength capacity which needs to be overcome before reaching complete collapse. Since such a restraining condition is not easily representable with the MB_P, both the 4-sides simply supported case and the 4-sides fixed supported case are simulated and reported in Table 6.

Table 6: Comparison between ELS and MB_P in terms of h water causing failure and y value

| Method used | h water causing failure | Point of application of the loading | y value |
|---|---|---|---|
| ELS | 2.65 m | 1/3h = 0.883 m | 1.275 m |
| MB_P – 4-sides fix supported case | 2.75 m | 1/3h = 0.916 m | 0.987 m |
| MB_P – 4-sides simply supported case | 2.10 m | 1/3h = 0.700 m | 0.759 m |

10

The results shown in Table 6 highlight that the ELS model can be better compared to a 4-sides fix supported case in the MB_P, as the variation in water height causing failure is only 3.77%, in comparison to the 4-sides simply supported case, for which the variation grows to 20.75%, thus confirming that the ELS model restraining conditions are more closely representable as fix supports. On the contrary, a very different trend is observed when considering the corresponding values of y. The result provided by ELS indicate that the position of maximum displacement is located at a distance equal to 1.275 m (i.e. approximately equal to half of the height of water causing collapse) and above the point of application of the loading. There is a substantial discrepancy between ELS and MB_P 4-sides fixed, with the latter being approximately 29.2% less: according to the MB_P the point of maximum displacement shifts down towards the base of the wall, still lying above the line of application of the loading profile. The case of MB_P – 4-sides simply supported case, which can be considered as the lower bound of this analysis, fails for a height of water that reaches 2.10 m. The position of y is still above the line of application of the loading, thus remaining consistent with the trend observed in previous cases considered.

## 4. Conclusions

The paper presents a mechanics-based procedure (MB_P) for the collapse load evaluation and failure mechanisms identification of brick masonry walls subjected to different types of hazards such as earthquake, flood and wind, and is part of wider multi-hazard assessment framework aiming to get to fragility assessment to complete the full risk assessment cycle. The procedure is tested to a masonry wall prototype and the set of assumptions adopted to conduct the analysis are reported. Two crack patterns are verified, with the aim of finding the "critical" crack configuration characterized by the lowest value of collapse load factor λ. Although aiming at "reducing" the number of assumptions individually related to each single hazard, some limitations related to the "pre-definition" of the crack pattern are found, with great attention posed to the case of flood loading. Further analyses are conducted to evaluate the flows of the procedure in that instance. A comparison is made between the wall simulated via a revised version of the MB_P that accounts for a reduced length of cracks dependant on the effective water height, and via the simplified micro-modelling approach ELS. The two parameters investigated and compared are the crack pattern and the position of maximum displacement of the point of convergence of cracks (i.e. y). The comparison shows good agreement in terms of crack pattern caused by very similar heights of water (differences in the range of 4%). However, in terms of y results, the ELS result is less conservative, and this is justifiable by the fact that the software can effectively capture the post-elastic behaviour of the wall, allowing to reach more extensive thresholds of displacement, in comparison to more conservative approaches like the MB_P proposed. The obtained results also must be interpreted in light of the fact that the crack pattern is an output in ELS, while it is an input for the MB_P. It is therefore justifiable that ELS provides with a failure pattern that represents the optimized solution among all possible patterns and a more precise estimation of the point of maximum displacement. Further research is required to address this issue for the case of earthquake and wind loading. Nonetheless, the MB_P shows good capabilities of capturing the behaviour of the wall under different types of loadings, with contained computational efforts required, which is ultimately the scope of multi-hazard vulnerability assessment procedures such as the one proposed in this study.

## 5. Acknowledgements

## 6. References

[1] Van Aalst, M. K. (2006). The impacts of climate change on the risk of natural disasters. Disasters, 30(1), 5-18.

[2] D'Ayala D. (2013) Assessing the seismic vulnerability of masonry buildings. Handbook of seismic risk analysis and management of civil infrastructure systems. Woodhead publishing, Oxford, pp 334–365

[3] D'Ayala D, Galasso C, Putrino V, et al (2016) Assessment of Multi-Hazard Vulnerability of Priority Cultural Her-itage Structures in the Philippines. In ICONHIC 2016, Chania, Greece.

[4] Delmonaco, G., Margottini, C., & Spizzichino, D. (2006). ARMONIA methodology for multi-risk assessment and the harmonisation of different natural risk maps. Deliverable 3.1. 1, ARMONIA

[5] Choine, M. N., O'Connor, A., Gehl, P., D'Ayala, D., García-Fernández, M., Jiménez, M. J., ... & Power, R. (2015, July). A multi hazard risk assessment methodology accounting for cascading hazard events. In 12th International Conference on Applications of Statistics and Probability in Civil Engineering, ICASP12 Vancouver, Canada (Vol. 20, pp. 12-15).

[6] Ingerslev, Å. (1923). The strength of rectangular slabs. Struct. Eng, 1(1), 3-14.

[7] Sinha, B. P. (1978). A simplified ultimate load analysis of laterally loaded model orthotropic brickwork panels of low tensile strength.

[8] Kelman, I., & Spence, R. (2003). A limit analysis of unreinforced masonry failing under flood water pressure. Masonry International, 16(2), 51-61.

[9] Herbert, D. M. (2013). An investigation of the strength of brickwork walls when subject to flood loading (Doctoral dissertation, Cardiff University).

[10] Vaculik, J. (2012). Unreinforced masonry walls subjected to out-of-plane seismic actions (Doctoral dissertation).

[11] Herbert, D. M., Gardner, D. R., Harbottle, M., & Hughes, T. G. (2018). Performance of single skin masonry walls subjected to hydraulic loading. Materials and structures, 51(4), 97.

[12] Herbert, D. M., Gardner, D. R., Harbottle, M., Thomas, J., & Hughes, T. G. (2011). The development of a new method for testing the lateral load capacity of small-scale masonry walls using a centrifuge and digital image correlation. Construction and Building Materials, 25(12), 4465-4476.

[13] Sorrentino, L., D'Ayala, D., de Felice, G., Griffith, M. C., Lagomarsino, S., & Magenes, G. (2017). Review of out-of-plane seismic assessment techniques applied to existing masonry buildings. International Journal of Architectural Heritage, 11(1), 2-21.

[14] Putrino, V., & D'Ayala, D. (2018, June). Mechanic-based Procedure for the Damage Mechanism Evaluation of Historic Masonry Structures. In Proceedings, 16th European Conference on Earthquake Engineering (Vol. 16). The European Association for Earthquake Engineering (EAEE).

[15] EN 1996-1 (2005) Eurocode 6: Design of masonry structures. Part 1: General rules for rein-forced and unreinforced masonry structures, CEN

[16] Cullen, A. C., Frey, H. C., & Frey, C. H. (1999). Probabilistic techniques in exposure assessment: a handbook for dealing with variability and uncertainty in models and inputs. Springer Science & Business Media.

[17] Tomaževič, M. (2009). Shear resistance of masonry walls and Eurocode 6: shear versus tensile strength of masonry. Materials and structures, 42(7), 889-907

[18] Simpson, R. H., & Saffir, H. (1974). The hurricane disaster potential scale. Weatherwise, 27(8), 169.

[19] ASI (2018): Extreme Loading for Structures V6. Applied Science International LLC, Durham, N.C., USA.

[20] Adhikari, R., & D'Ayala, D. (2019, June). Applied Element Modelling and Pushover Analysis of Unreinforced Masonry Buildings with Flexible Roof Diaphragm. In 7th (ECCOMAS).